Synovial immune endotypes associate with structural severity across canine and human osteoarthritis.

Authors: Anaëlle Drieu-Vincent[1†], Julien De Lima[2†], Floriane Etienne[2], Romain Guiho[2], Noémie Podevin[1], Richard Danger[3], Florence Lezin[4], Nicolas Gaigeard[2], Sophie Allain[2], Jérôme Abadie[4], Thomas Rousseau[1], Pierre Maitre[1,2], Olivier Gauthier[1,2], Jérôme Guicheux[2], Marion Fusellier[1,2††*], Marie-Astrid Boutet[2††*].

SUPPLEMENTAL FIGURES AND TABLES

Supplemental Table 1: MRI sequences and acquisition parameters for canine stifle imaging.

MR sequence	TR (ms)	TE (ms)	FOV (mm)	Matrix	Voxel size (mm)	Slice Thickness (mm)	Interslice Gap (mm)
Sag T1w TSE	433	12	180	384 x 384	0.46 x 0.46 x 2.5	2.5	0.375
T2w 3D TSE	1100	149	160	512 x 512	0.31 x 0.31 x 0.36	0.36	0
T1w 3D VIBE with water excitation fat suppression	16.9	7.26	160	512 x 512	0.31 x 0.31 x 0.3	0.3	0
Sag PD FAT-SAT BLADE	1900	55	180	512 x 512	0.35 x 0.35 x 2.5	2.5	0.3

Sagittal Localizer (Sag Localizer) was used only for stifle orientation.
TR = Time of Repetition; ms = milliseconds; TE = Time of Echo; FOV= Field-of-view; Sag = Sagittal; T1w = T1-weighted; TSE = Turbo Spin Echo; T2w = T2-weighted; 3D = three dimensional; VIBE =Volumetric Interpolated Breath-hold Examination; PD = Proton Density; FAT-SAT = Fat-Saturation; BLADE refers to a Siemens rotating phase-encoding sequence.

Supplemental Table 2. MRI scoring of osteoarthritis lesions in the canine stifle.

Structure	Feature	Score	Description
Cartilage	Cartilage signal	0	Normal signal
		1	T2 hyperintensity
	Cartilage lesions [43]	0	No abnormality
		2.0	Focal lesion, partial thinning involving <10% of the affected region
		2.5	Focal lesion, full-thickness thinning involving >10% of the affected region
		3	Multiple grade 2.0 lesions with normal thickness areas, or grade 2.0 involving > 10% but <75% of the region
		4	Diffuse lesions with partial thinning (≥75% of the region)
		5	Multiple grade 2.5 lesions, or grade 2.5 lesions involving > 10% but <75% of the affected region
		6	Diffuse full-thickness lesions (≥75% of the region)
Subchondral bone	Subchondral edema	0	Absent
		1	<25% of the affected region
		2	25%-50% of the affected region
		3	>50% of the affected region
	Subchondral cysts	0	Absent
		1	Mild
		2	Moderate
		3	Severe
Osteophytes	-	0	Absent
		1	Mild
		2	Moderate
		3	Severe
Ligaments	Ligament lesions and signal [43]	0	Ligament normal, continuous, regular thickness, normal signal, no edema or hyperintensity
		1	Ligament continuous, normal signal but with intraligamentous signal increase
		2	Ligament thinned or elongated but continuous (partial rupture)
		3	Ligament absent or completely ruptured
	Ligament thickening	0	Absent
		1	Present
Menisci	Meniscal morphology	0	No abnormality
		1	Intrameniscal hyperintensity without surface extension
		2	Horizontal tear
		3	Radial or vertical tear
		4	Bucket-handle tear, displaced tear, or complex tear
		5	Partial maceration/destruction
		6	Total maceration
	Meniscal extrusion	0	No extrusion

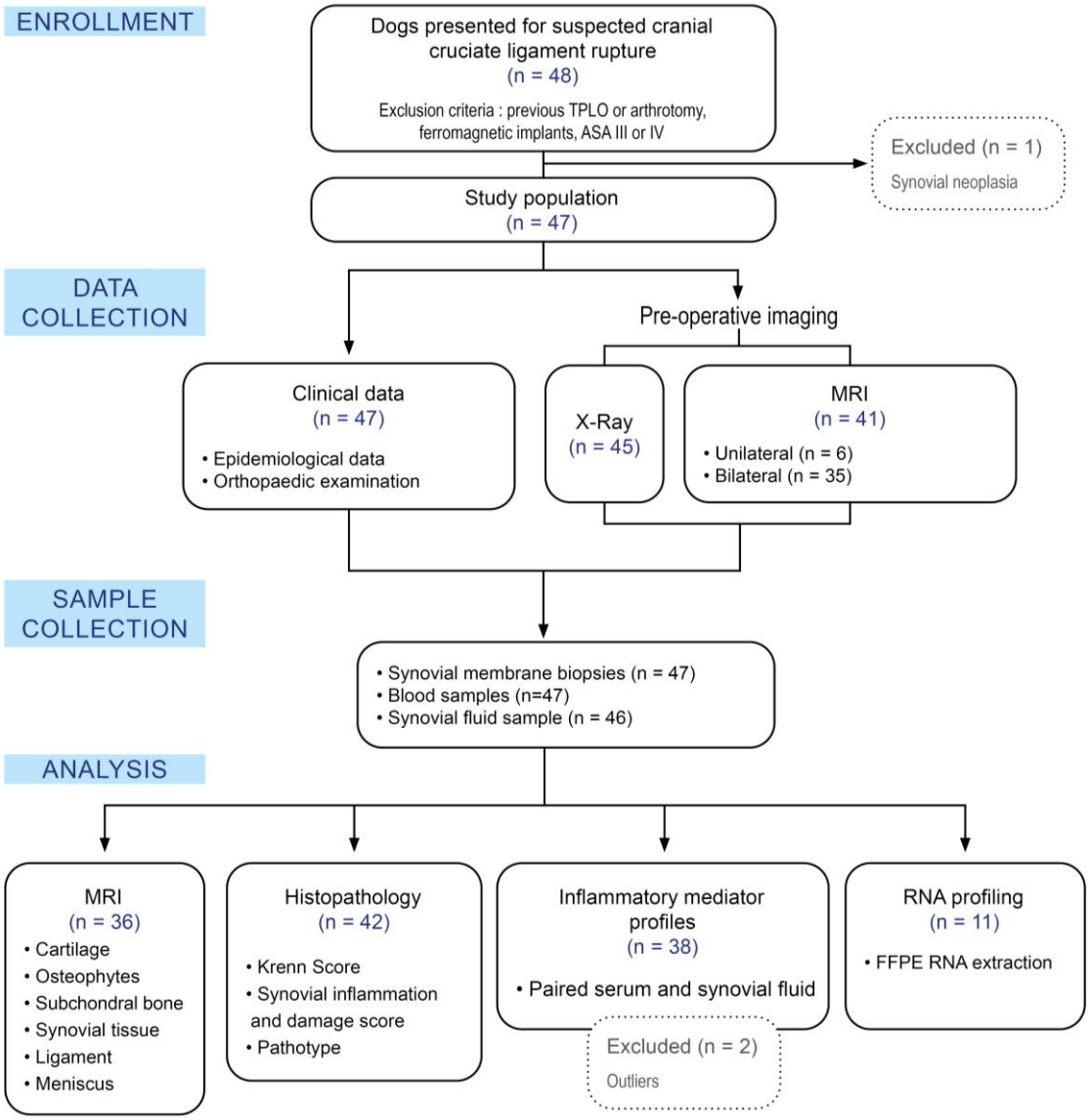
		1	Extrusion <50% of meniscal length (Coronal view)
		2	Extrusion ≥50% of meniscal length
Synovium	Synovitis	0	<2 mm
		1	2-4 mm
		2	>4mm
	Synovial villi	0	Absent
		1	Present
	Synovial cysts	0	Absent
		1	Present
Synovial fluid	-	0	No signal abnormality
		1	Intermediate signal on T1w or T2w sequences
Joint capsule	-	0	Physiological
		1	Mild
		2	Moderate
		3	Severe
Additional abnormalities	Tenosynovitis of the common digital extensor tendon	0	Absent
		1	Present
	Popliteal lymphadenopathy	0	Absent
		1	Present

Cartilage signal was evaluated on T2-weighted 3D TSE sequences [44]; morphology and lesions on T1-weighted 3D VIBE with water excitation fat suppression sequences. Bone marrow lesions (edema and cysts) were assessed on T1-weighted 3D VIBE [D'anjou M-A and al. DOI:10.1016/j.joca.2008.03.022]. Osteophytes were scored on T1-weighted 3D VIBE and T2-weighted 3D TSE [45]. Ligament continuity, signal, and thickening were evaluated on T1-weighted 3D VIBE. Meniscal morphology and extrusion were assessed using PD FAT-SAT BLADE and T2-weighted 3D TSE [43]. Synovitis, synovial villi, cysts, joint capsule distension, and synovial fluid signal were evaluated on PD FAT-SAT BLADE, T2-weighted 3D TSE, and T1-weighted TSE [Perry TA and al. DOI:10.1093/rheumatology/keaa619, 46]. Other abnormalities were recorded on PD FAT-SAT BLADE and T2-weighted 3D TSE.

Supplemental Table 3. Radiographic grading of the canine osteoarthritic stifle

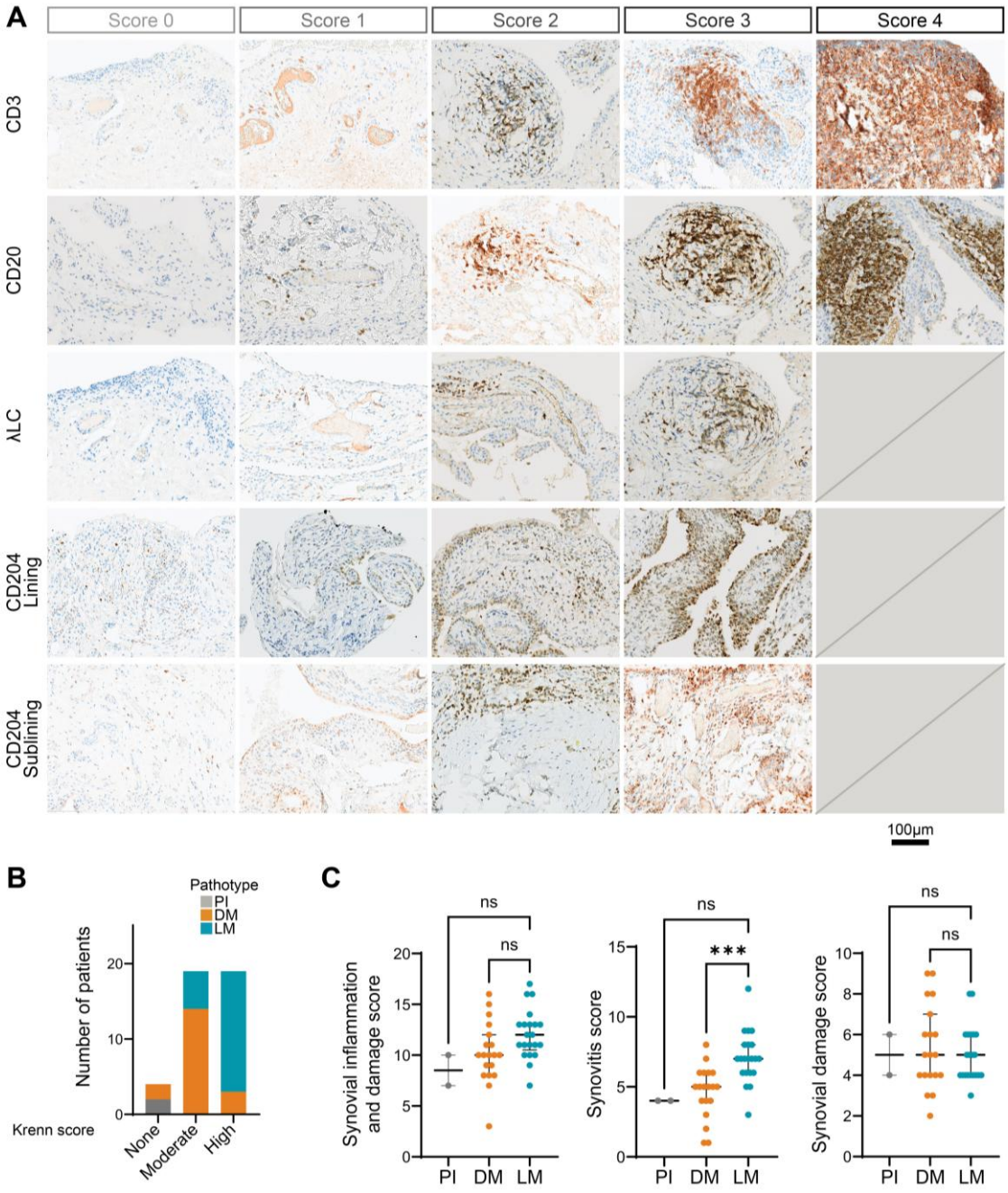
Grade	Description
0	No radiographic signs of OA
1	Minimal changes: small osteophytes and/or minimal joint space narrowing
2	Mild OA: definite osteophytes with mild joint space narrowing
3	Moderate OA: marked joint space narrowing associated with subchondral sclerosis, remodeling and/or subchondral cysts

Supplemental Figure 1



Supplemental Figure 1: Study flow chart. TPLO: Tibial Plateau Leveling Osteotomy.

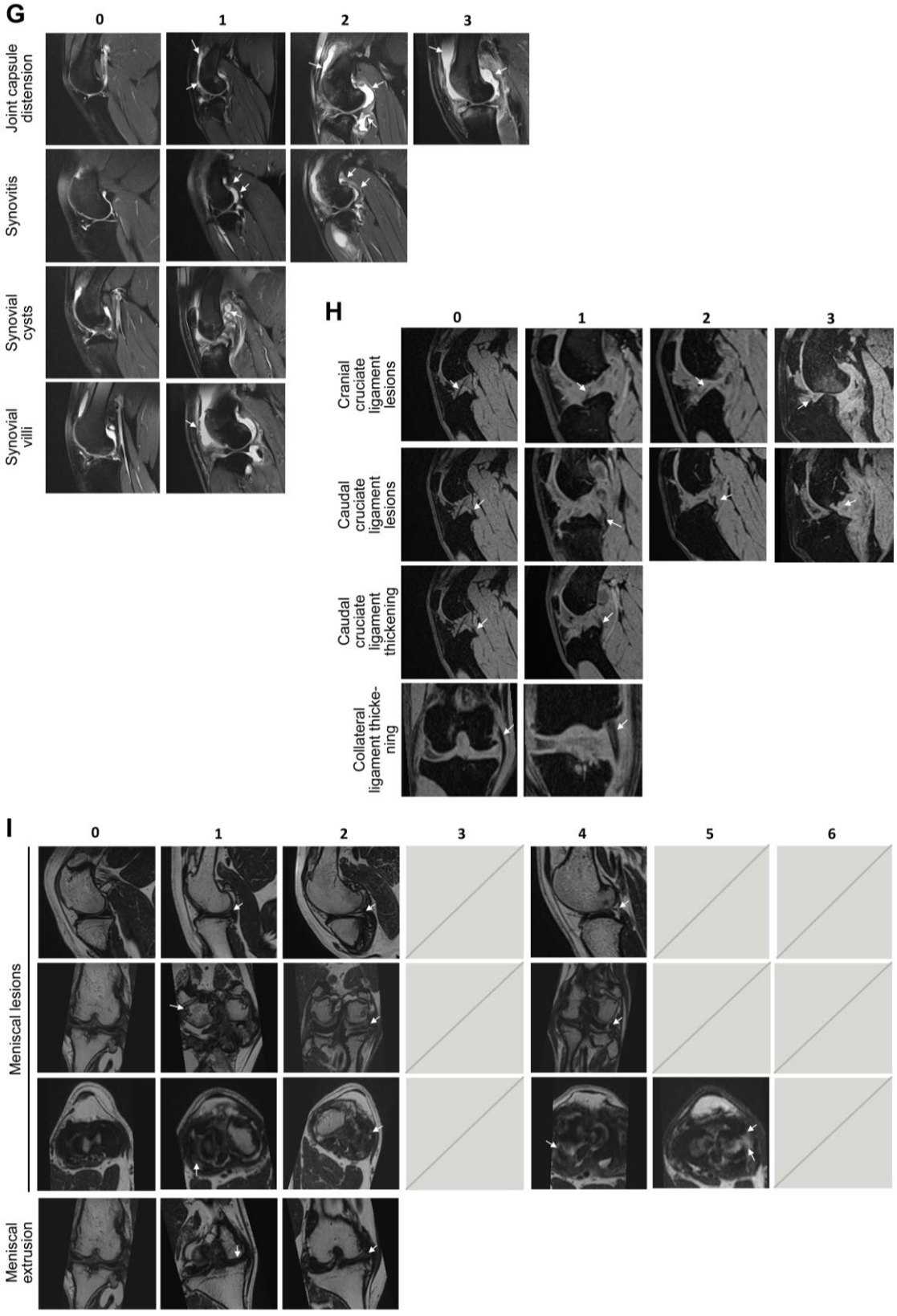
Supplemental Figure 2



Supplemental Figure 2: Pathotype classification in canine OA. ***Associated with main Figure 1.*** **(A)** Representative images of synovial tissues illustrating the scoring scale (0–4) for each immunohistochemical marker: CD3 (T cells), CD20 (B cells), lambda light chain (λLC; plasma cells), and CD204 (macrophages) in the lining and sublining layers. Scale bar = 100 µm. **(B)** Bar chart representing the distribution of Krenn's categories in each pathotype group in synovium from canine OA patients (n=42). **(C)** Graphs representing the distribution of synovial inflammation and damage histological scores in each pathotype group in synovium from canine OA patients (n=42). Statistical comparisons were performed using Kruskal-Wallis test and Dunn's posttest. ***, p-value < 0,001; ns, not significant; each dot represents an individual.

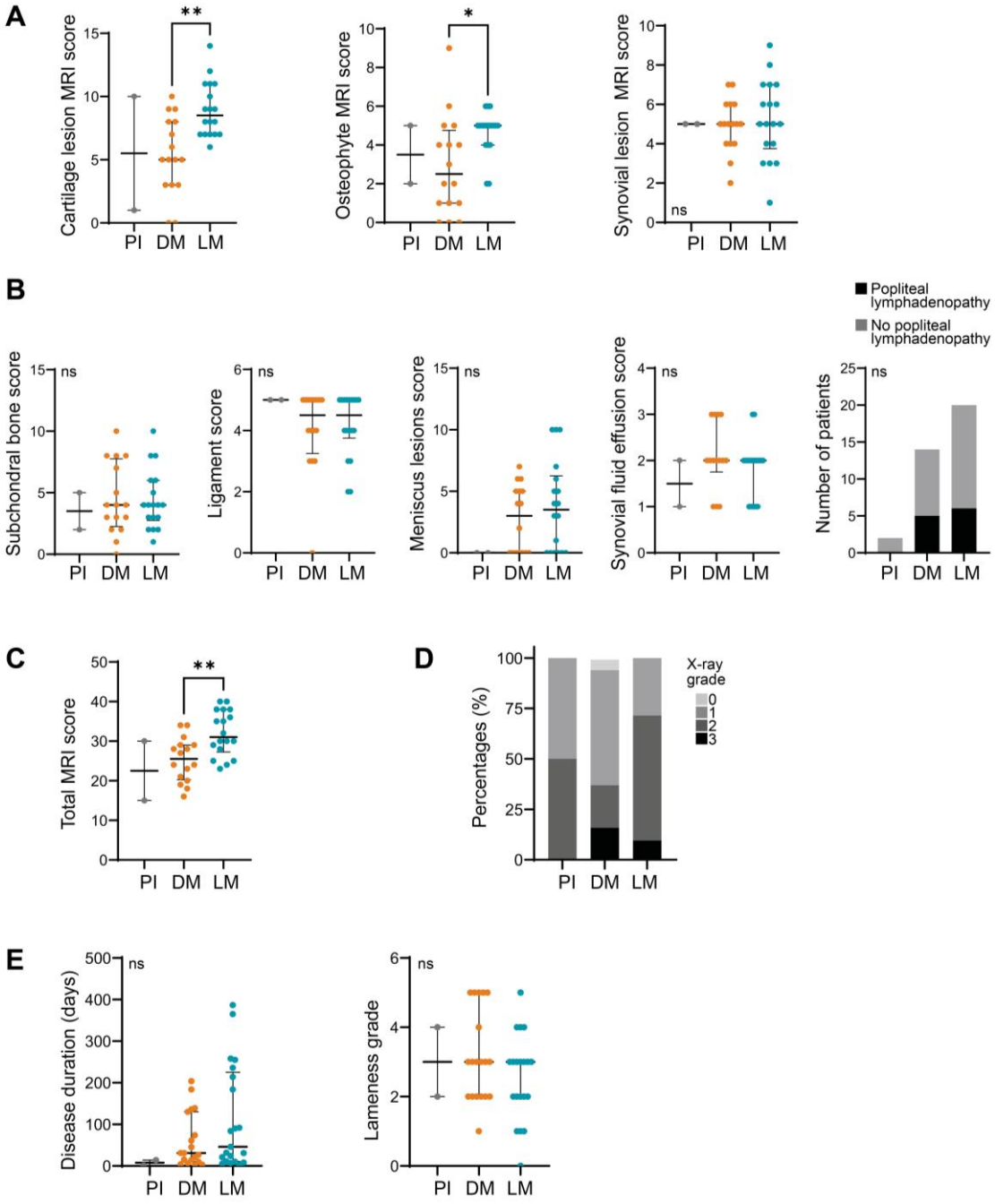
Supplemental Figure 3




G
0
1
2
3
Joint capsule distension
Synovitis
Synovial cysts
Synovial villi
H
0
1
2
3
Cranial cruciate ligament lesions
Caudal cruciate ligament lesions
Caudal cruciate ligament thickening
Collateral ligament thickening
I
0
1
2
3
4
5
6
Meniscal lesions
Meniscal extrusion

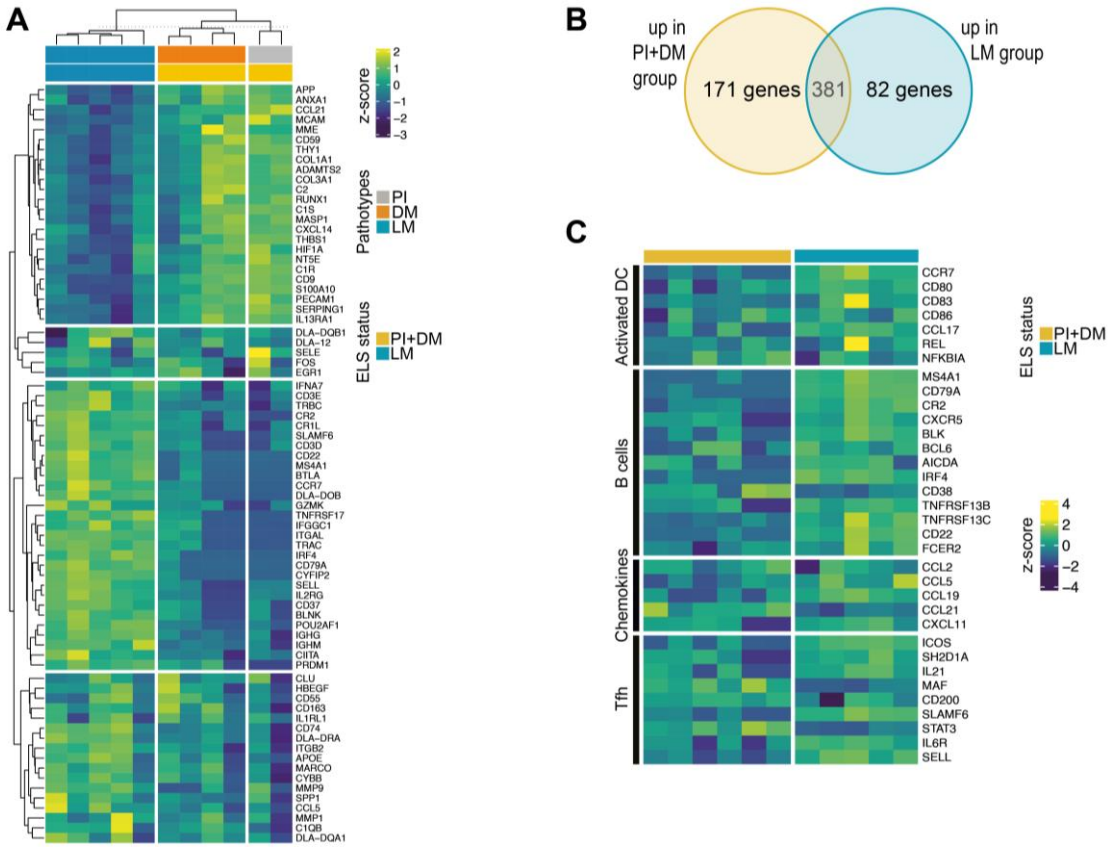
Supplemental Figure 3: MRI scores of canine OA joint. ***Associated with main Figure 2*****. (A-I)** Representative MRI images illustrating the scoring scale attributed for the following criteria: cartilage lesions (including cartilage edema and signal abnormalities) **(A, B)**, osteophytes **(C)**, subchondral lesions (including subchondral bone edema and subchondral bone cysts) **(D)**, other lesions (including tenosynovitis, synovial fluid signal abnormalities and popliteal lymphadenopathy) **(E, F)**, synovial lesions (joint capsule distension, synovitis, synovial cysts and villi) **(G)**, ligament lesions (cranial and caudal cruciate ligament lesions, caudal and collateral ligament thickening) **(H)** and meniscal lesion (meniscal morphology and extrusion) **(I)**. White arrows indicate the lesion.

Supplemental Figure 4



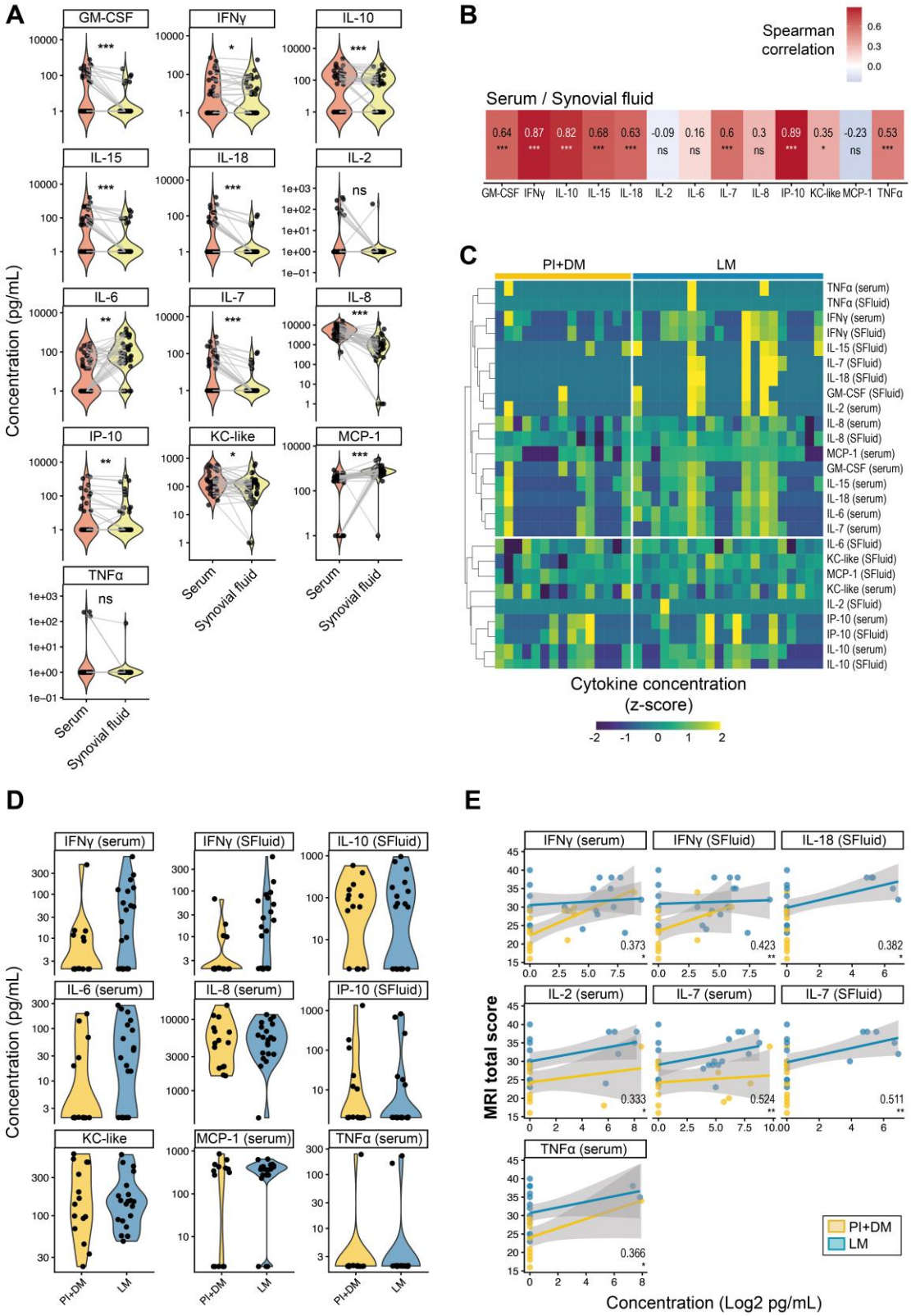
Supplemental Figure 4: Lympho-myeloid synovial pathotype is associated with more severe MRI-detected joint damage in canine OA. ***Associated with main Figure 2*. (A)** Graphs representing the distribution of cartilage lesion (left panel), osteophyte (middle panel), synovial lesion (right panel) scores in patients presenting a pauci-immune (PI), diffuse-myeloid (DM), or lympho-myeloid (LM) pathotype. **(B)** Subchondral bone, ligament, Meniscus lesion and synovial effusion MRI scores (left panels) and repartition of popliteal lymphadenopathy (right panel) in patients presenting a PI, DM or LM pathotype. **(C)** Total MRI scores in patients presenting a PI, DM or LM pathotype. n= 36 **(D)** Bar chart representing the distribution of X-ray grades (0-3) across different histopathological groups (PI, DM and LM). n= 42 **(E)** Graphs representing disease duration in days (left panel) and lameness grade in PI, DM and LM groups. n= 42 **(A-E)** Each dot represents one stifle. Median and interquartile range are shown. Statistical comparisons were performed using Kruskal-Wallis test and Dunn's posttest. *, p-value < 0.05; **, p-value < 0.01; ns, not significant.

Supplemental Figure 5



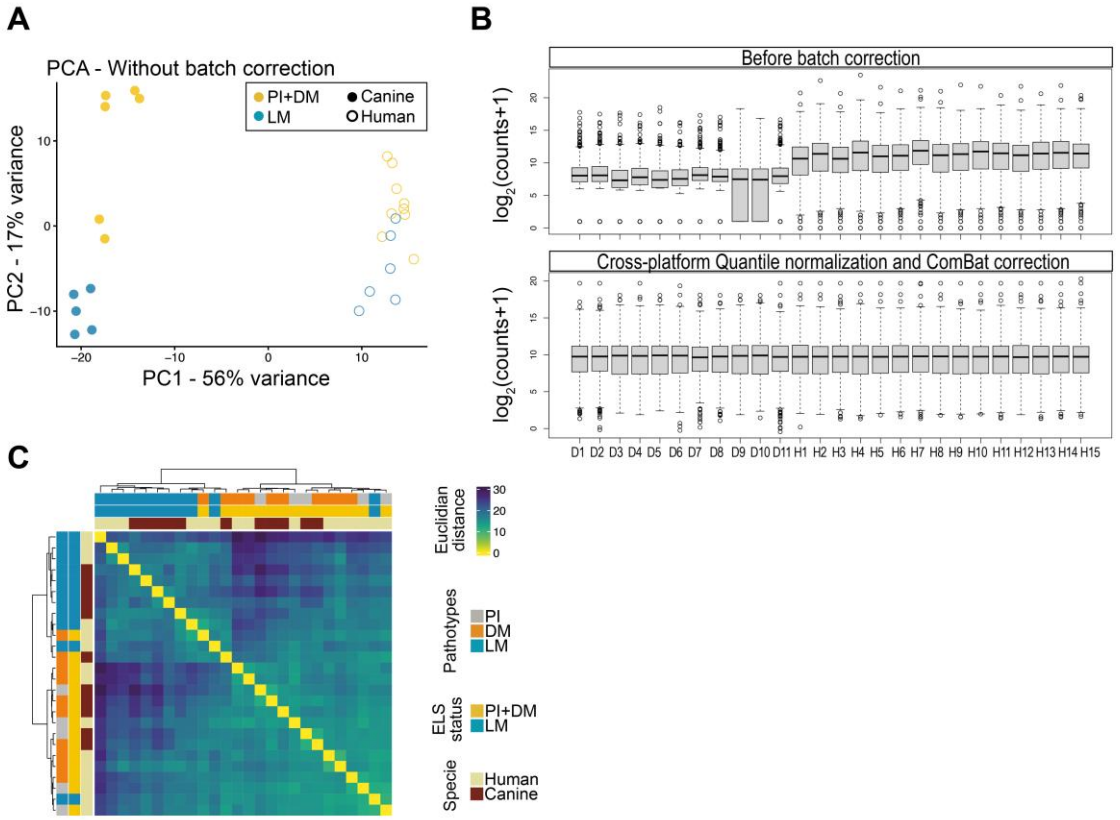
Supplemental Figure 5: Canine OA synovial pathotypes define distinct immune endotypes with specific transcriptomic programs. ***Associated with main Figure 3*****. (A)** Heatmap of differentially expressed genes across the three synovial pathotypes (PI, DM and LM) or groups (LM versus PI+DM). Each row represents a gene, and each column corresponds to an individual patient (n=11). The yellow/blue scale represents the normalized z-scores of gene expression, unsupervised clustering. **(B)** Venn diagram representing the number of common (n=381) and specific genes in each group (PI+DM, n=171 versus LM, n=82). **(C)** Heatmap of differentially expressed genes belonging to the ectopic lymphoid structure (ELS) signature, including genes characteristic of activated dendritic cells (DCs), B cells, chemokines, and follicular helper T cells (Tfh). Each row represents a gene, and each column corresponds to an individual patient (n=11). The yellow/blue scale represents the normalized z-scores of gene expression.

Supplemental Figure 6



Supplemental Figure 6: Inflammatory mediator profiles in serum and synovial fluid correlate with clinical and imaging parameters. ***Associated with main Figure 4*****. (A)** Violin plot representing the cytokine concentration in pg/mL comparatively in serum and synovial fluids. Statistical comparisons were performed using the paired Wilcoxon test. *, p-value < 0.05; **, p-value < 0,01; ***, p-value < 0,001; ns, not significant; each dot represents an individual. n=36. **(B)** Spearman correlation coefficient between serum and synovial fluid values for each analyte analyzed. Statistical comparisons were performed using the Spearman correlation test. *, p-value < 0.05; ***, p-value < 0,001; ns, not significant. **(C)** Heatmap of cytokine concentrations, each row represents an analyte, and each column corresponds to an individual patient (grouped in pauci-immune and diffuse-myeloid PI+DM in yellow, and lympho-myeloid LM in blue). The scale represents the normalized z-scores of concentrations. **(D)** Violin plot representing the cytokine concentration in pg/mL comparatively in PI+DM (yellow) and LM (blue) groups. Each dot represents an individual. **(E)** Correlation plots showing the relationship between cytokine concentrations (log2-transformed pg/mL) and total magnetic resonance imaging (MRI) score. Each dot represents one patient. Linear regression lines with 95% confidence intervals are shown separately for the PI+DM group (yellow) and the LM group (blue). Spearman correlation coefficients and associated p-values were calculated for each cytokine across the full cohort and are indicated on the graphs. *, p-value < 0.05; **, p-value < 0,01.

Supplemental Figure 7



D

Up in PI+DM group

Human DEGs			Canine DEGs		Core signature
ABCF1	MTOR	ERBB3	ABL1	PCNA	ABL1
ABL1	NDRG1	ITGA2	ACVR1	PDGFC	ADAMTS2
ADAMTS2	NF1	MAP2	ADAMTS2	PECAM1	AKT3
AKT1	NFATC1	RAG2	AKT3	PLCG1	APP
AKT3	NFATC4		APP	PNMA1	BCR
APP	NOD1		ATG16L1	PRKCE	BRAF
AXL	NOTCH1		ATG7	PTK2	C6
BCL6	NRDE2		BCR	PUM1	CCL21
BCR	PDGFRA		BRAF	RORA	CD276
BRAF	PDGFRB		BRCA2	S100A10	CD34
C6	PIK3C2B		BST1	SERPING1	CDH5
CCL14	PIK3R1		C1S	SHMT2	COL3A1
CCL21	PLCG1		C6	SRC	ERBB2
CD276	PRKCE		CASP10	STAT5B	ERCC3
CD34	PUM1		CCL21	TBK1	IGF1R
CD81	RELA		CCND1	TGFB2	IL7
CD99	RORA		CD276	TRAP	ITGA1
CDH5	SDC4		CD34	TNFRSF1A	ITGB3
CEACAM1	SERPING1		CD59	TNFSF12	JAM3
CNP	SF3A1		CD9	TNKS2	LTBR
COL3A1	SMARCA4		CDH5	TYMS	MASP1
CREBBP	SPRY2		CHUK	ZEB1	MCAM
DNMT3A	SRC		CMA1	CLDN1	MTOR
DUSP1	STAT5B		COL1A1	GH1	NF1
EGFR	STK11		COL3A1	IL17RB	NFATC4
EGR1	TFE3		DOK1	KIT	NOD1
ERBB2	TFEB		ERBB2	TAL1	PLCG1
ERCC3	TGFB1		ERCC3	CASP8	PRKCE
ESR1	TNFRSF1A		FBXW11	CLEC4A	PUM1
ETS1	TNFSF12		GSK3B	FLT3LG	RORA
FAT1	TRAF2		HRAS	PLAUR	SERPING1
FGFR1	TSC2		IDH1	RET	SRC
FOS	TYK2		IFNAR1	SLC16A1	STAT5B
GPI	VIM		IGF1R	MASP2	TNFRSF1A
GSK3A	ZEB1		IGF2R	ATG10	TNFSF12
IGF1R	AR		IL11RA	CSF2	ZEB1
IKBKG	CD200		IL13RA1	IDO2	TAL1
IL17RA	TAL1		IL13RA2	IL25	FLT3LG
IL6ST	FLT3LG		IL4R	IL34	IL25
ILF3	IL1RL2		ILF3	NLRP3	ABCB1
INPPL1	PRG3		ITGA1	NPNT	POLR1G = CD3EAP
ITGA1	PGR		ITGA6	ABCB1	ITGA2
ITGA5	TCF7		ITGB3	BIRC5	MAP2
ITGB3	C9		JAM3	CD3EAP	RAG2
JAM3	CCR6		LTBR	FPR2	
KDR	CCR9		MAF	ITGA2	
KMT2A	CX3CL1		MAP2K1	MAP2	
KMT2D	IL13		MAP2K4	MGMT	
LAMP1	IL5		MAP3K7	RAG2	
LCN2	KLRA1P		MAPK8	TNFSF4	
CTSV	MST1R		MASP1		
LTBR	AICDA		MCAM		
MAP2K2	ARG1		MME		
MAP4K2	CCR7		MTOR		
MAPK3	DMBT1		NF1		
MASP1	IL25		NFATC4		
MAVS	ABCB1		NOD1		
MCAM	POLR1G		NRP1		

Up in LM group

Human DEGs			Canine DEGs			Core signature
ATF1	MAF	CCL13	ALCAM	SYK	TLR10	BTK
ATF2	MAP2K4	CD3D	BTK	TAP1	TNFRSF17	C1QA
ATG5	MIF	CD8A	C1QA	TFEB	TRAC	C1QB
ATG7	MME	CTLA4	C1QB	TLR1	ADORA2A	C3AR1
B2M	MMP1	EOMES	C3AR1	TNFAIP3	BTLA	CCR1
BID	MRC1	GBP5	CCR1	TNFRSF13C	CD22	CD180
BST1	MS4A2	GZMB	CD180	TNFRSF1B	CD3G	CD53
BST2	MSR1	IL21	CD47	TNFSF13	CD79A	CFB
BTK	NCF4	CD200R1	CD53	TNFSF13B	CYFIP2	CTSH
C1QA	NRAS	POU2AF1	CD68	TRAF3	IRF4	CTSS
C1QB	OAS2	PRDM1	CD74	TRIB1	LOC484343	HLA-F = DLA-79
C1QBP	OAZ1	SLAMF6	CD83	CITA	MS4A1	HLA-B = DLA88
C3AR1	PCNA	SLAMF7	CEACAM1	IGHG	POU2F2	HLA-DMA = DLA-DMA
CASP10	PSMB8	BLK	CFB	IGHM		HLA-DMB = DLA-DMB
CASP3	PSMB9	CD2	CTSH	IRF8		HLA-DRA = DLA-DRA
CCL2	PTPRC	HLA-DOB	CTSS	TLR6		EPSTI1
CCR1	PYCARD	GZMH	CYBB	TRAF1		IL18
CD14	RB1	ICOS	DLA-79	TRBC		LCP1
CD180	RPS6	ISG15	DLA88	CCL20		FCGR3A = LOC478984
CD209	S100A10	ITGAL	DLA-DMA	CCL5		LYN
CD38	S100A4	TNFRSF17	DLA-DMB	CD3E		MRC1
CD53	SPP1	TRAC	DLA-DRA	CD48		NCF4
CD58	STAT1	ANKRD22	DOCK2	CD5		PSMB8
CD63	SYK	CD28	EPSTI1	CR1L		PSMB9
CD86	TANK	CD79A	FAS	CXCR4		PTPRC
CDK4	TAP1	FPR2	FN1	GZMK		PYCARD
CFB	TLR1	HAVCR2	ICAM2	IL2RG		SPP1
CHUK	TLR2	IL1B	IKBKB	IL6R		SYK
CPA3	TLR4	IRF4	IKBKE	ISG20		TAP1
CTSH	TLR7	MS4A1	IL10RA	ITGB2		TLR1
CTSS	TLR8	S100A12	IL18	LOC102153988		TNFSF13
HLA-F	TNFSF13	S100A9	IRF1	PIK3CG		TNFSF13B
HLA-B	TNFSF13B		IRF2	SELL		IGHG1 = IGHG
HLA-DMA	TREM2		ITGAX	TCF7		IGHM
HLA-DMB	TYROBP		JAK3	TNFRSF13B		TRBC1 = TRBC
HLA-DRA	CCR2		LAIR1	BLNK		CD3E
EPSTI1	CCR5		LCP1	CCL19		CD48
F13A1	FLT3		LOC478984	CCR6		IL2RG
FCER1G	IFIT2		LOC484306	CD37		CXCL1 = LOC102153988
FCGR1A	IGHG1		LYN	CD3D		PIK3CG
HCK	IGHM		MAP3K1	CR2		SELL
IDH1	KIT		MAP4K2	EOMES		CD3D
IFI35	LY86		MEF2C	IL21R		EOMES
IFIH1	S100A8		MRC1	POU2AF1		POU2AF1
IFNGR1	TRBC1		NCF4	PRDM1		PRDM1
IL10	CALHM6		NFKB2	SLAMF6		SLAMF6
IL18	CD3E		NLRC5	SLAMF7		SLAMF7
IRAK4	CD48		NR1H3	STAT4		BLK
JAK2	CD80		PDPN	BLK		CD2
LAMP2	CLEC4A		PIK3C2B	CCR7		HLA-DOB = DLA-DOB
LAP3	FASLG		PRKCD	CD2		ICOS
LCP1	IL2RG		PSMB8	CFP		ISG15
LGALS1	CD33		PSMB9	DLA-DOB		ITGAL
LGALS3	CXCL1		PTPRC	ICOS		TNFRSF17
FCGR2B	XCL1		PYCARD	IL1R2		TRAC
FCGR3A	PIK3CG		SELPLG	ISG15		CD79A
LY96	SELL		SPP1	ITGAL		IRF4
LYN	TRGC2		STAT2	LY9		MS4A1

Supplemental Figure 7: Multimodal cross-species analyses uncover conserved synovial immune features and actionable therapeutic targets in OA. ***Associated with main Figure 5*****. (A)** Principal component analysis (PCA) presenting the distribution of dog patients (plain dots, n= 11) and human patients (empty dots, n = 15), according to their histopathological group ("PI+DM" ellipse in yellow, "LM" ellipse in blue) before batch correction. Ellipses indicate the 95% confidence interval for each group and axes represent principal components 1 and 2, explaining 56% and 17% of the total variance, respectively. **(B)** Bar plot representing log2(counts+1) before batch correction (upper panel) and after quantile normalization and ComBat correction for each dog (D) and human (H) patient. **(C)** Sample-to-sample Euclidean distance heatmap of cross-species transcriptomic profiles. Samples are annotated by species and pathotype groups. Lower distances (lighter colors) indicate higher transcriptomic similarity, whereas higher distances (darker colors) indicate greater divergence. **(D)** List of human and canine-specific and common (core signature) differentially expressed genes (DEG) up in PI+DM (left panel) and LM (right panel) groups.